

A Review of Candidate Ceramic Materials for Use as Heat Shield Tiles in a Supercritical-Water-Cooled-Reactor

Peter McClure, Blaine Geddes, Xiao Huang and Dave Guzonas*

Dept. of Mechanical and Aerospace Engineering

Carleton University

*Atomic Energy of Canada Limited

Abstract

The proposed Canadian supercritical-water-cooled reactor (SCWR) utilizes a reactor shell made of a zirconium alloy insulated with a ceramic tile heat shield. The main consideration in the selection of a tile material will be resistance to corrosion in supercritical water and long term microstructure stability, in addition to thermal conductivity. This paper provides a review of the literature on corrosion behaviours of ceramic materials in supercritical water and ranks candidate ceramic materials accordingly. Materials reviewed include alumina, zirconia, silica glasses, silicon carbide, silicon nitride, sialon, mullite, and aluminum nitride.

1. Introduction

The proposed Atomic Energy of Canada Limited (AECL) generation four nuclear reactor (Gen IV) is a supercritical-water-cooled reactor (SCWR), with the reactor shell made of a zirconium alloy insulated with a ceramic tile heat shield. The heat shield must provide a temperature drop from the internal supercritical water temperature (between 650°C and 750°C) to a level acceptable for long term operation of the chosen zirconium alloy. The thickness of the tiles will be determined by their thermal conductivity and the required temperature drop. The tiles will be mounted using perforated liner such that they will carry only the hydrostatic compressive stress of the reactor operating pressure, on the order of 25 MPa. The main consideration in the selection of a tile material will be resistance to corrosion in supercritical water and long term microstructure stability. This paper provides a review of the literature on corrosion behaviours of ceramic materials in supercritical water and ranks candidate ceramic materials accordingly.

2. Corrosion in Supercritical Water

Water reaches a supercritical state at a temperature above 374°C and a pressure above 22.05 MPa. Supercritical fluids have properties between those of a gas and a liquid, analogous to a dense gas. The density and ionic dissociation of water drops significantly above the transition point to supercritical state. Increased pressure makes the shift in physical properties more gradual and moves the transition point to a higher temperature. Figure 1 shows the drop in ionic product and density of water at pressures of 24 MPa and 38 MPa.

The shift in physical properties significantly affects the corrosion characteristics, with water varying from a solvent of high density and polarity solvent, to low density and polarity. In general, corrosion rates rise with temperature as reaction and diffusion rates increase. When

water changes to a supercritical state, however, the nature of corrosion is changed. The corrosion rate of supercritical water has been shown to be significantly lower than that of near-critical water [1]. Figure 2 shows the effect of temperature on corrosion rate based on experiments using a very weak HCl solution containing high levels of dissolved oxygen.

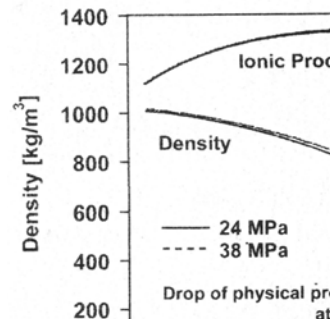


Figure 1 - Drop in physical properties of water with temperature [1]

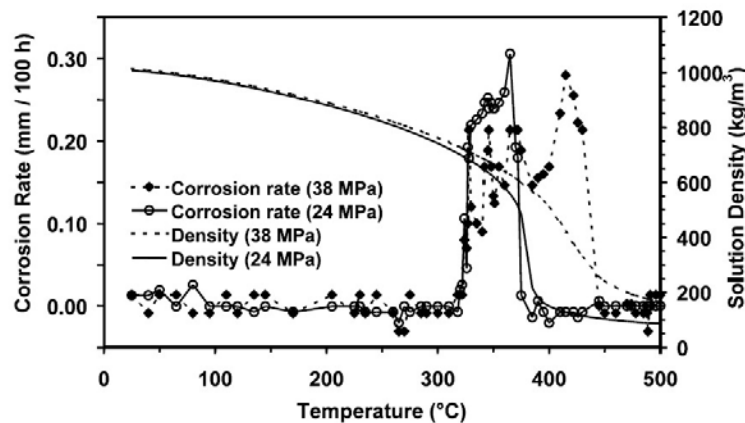


Figure 2 - Corrosion rate and density changes of water with temperature [1]

Two observations can be made from this experiment. Corrosion rate increases significantly near 320°C, regardless of pressure, and returns to low temperature rates as the water reaches a supercritical state. This is due to the drops in density and ionic product, seen in Figure 1, as low density low polarity fluids are less conducive to corrosion [1]. Corrosion rate of a fluid can thus be correlated with density, with the divide between low and high corrosion fluids at approximately 250 kg/m³[1]. Figure 3 shows the variation in density as a function of fluid temperature and pressure.

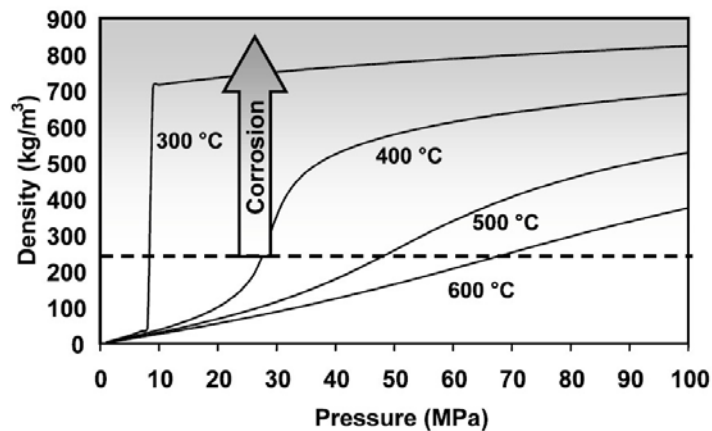


Figure 3 - Density of high temperature water as a function of pressure [1]

As seen in this figure, water at temperatures above the supercritical point (374°C at 22.05 MPa) tends to have a low corrosion rate compared to near-critical temperatures and pressures.

3. Ceramics in Supercritical Water

A comprehensive test of corrosion of ceramic materials in supercritical water was performed in 1997 [2]. Ceramics were exposed to supercritical water (with 0.05 mol/kg HCl and 3% H₂O₂) at 465°C and 25 MPa for up to 220 hours. Corrosion rate and corroded layer from this testing for the candidate ceramics discussed in this report are shown in Table 1, as are key properties of the materials. This is not an exhaustive list of ceramic materials, but rather ceramic materials were selected as reasonable potential candidates for consideration, or materials for which literature was available.

Table 1 - Corrosion performance and key properties for candidate ceramic materials [2][3]

Material	Corrosion Performance			Key Physical Properties			
	Exposure Time (hr)	Corrosion Rate (mg/cm ²)	Corroded Layer (µm)	Thermal Conductivity (W/m-K)	Thermal Expansion Coeff. (10 ⁻⁶ /°C)	Elastic Modulus (GPa)	Flexural Strength (MPa)
Al ₂ O ₃ (99.7%)	220	<0.1	<10	18	8.1	300	330
ZrO ₂ (96.5 mol%, 3.5 mol% MgO)	220	<0.1	<10	2	10.3	200	900
SiO ₂	n/a	n/a	n/a	1.4	0.55	73	
SiC (S-SiC)	133	75		120	4	410	550
Si ₃ N ₄ (99%, free Si <1%)	144	129.49	<10	30	3.3	310	830
Sialon (Si _{5.3} Al _{0.7} O _{0.7} N _{7.3})	150	74.19	400	15-20	3	288	760
Mullite (70%, 10% SiC, 15% ZrO ₂ , 5%Al ₂ O ₃)	144	2.28	170-220	6	5.4	151	180
AlN	80	-4.83 (weight gain)		140-180	4.5	330	320

From these results, alumina (Al_2O_3) and zirconia (MgO stabilized ZrO_2) show the most promise for use in supercritical water, while mullite and aluminum nitride (AlN) may also be feasible, but were not tested for the entire 220 hours. Aluminum nitride actually shows a negative corrosion rate due to a layer of protective alumina forming on the surface. Further analysis of individual candidate ceramic materials is summarized below.

3.1 Alumina – Al_2O_3

High purity alumina has excellent resistance to corrosion, but degrades with the addition of impurities due to attack at the grain boundaries where impurities are segregated. Testing by Oda and Yoshia[4] of alumina corrosion in subcritical water at a temperature of 300°C and 8.6 MPa for 1 to 10 days shows the effect impurities have on the corrosion rate. Three samples were tested: 99% alumina, 99.9% alumina and 99.99% alumina. Compositions of the three specimens are given in Table 2.

Table 2 - Composition of alumina specimens [4]

Specimen	Al_2O_3	SiO_2	Na_2O	MgO	CaO	Fe_2O_3	Density (g/cm^3)	Flexural Strength (MPa)
2N	98.7	1.17	0.09	0.01	0.03	<0.01	3.84	304
3N	99.92	0.04	0.02	0.01	0.01	<0.01	3.93	490
4N	99.98	0.01	0.01	<0.01	<0.01	<0.01	3.95	588

The weight loss of the specimens was measured over time and found to be mainly due to the dissolution of SiO_2 and Na_2O which were present as impurities in the alumina primarily at the grain boundaries. Figure 4 shows weight loss of the specimens as a function of time. A significant difference is seen in the corrosion rates between the 99% sample and the 99.9% sample, but much less difference in corrosion rates between the 99.9% sample and the 99.99% sample - corrosion rate was approximately linear with sample purity for these high purity samples.

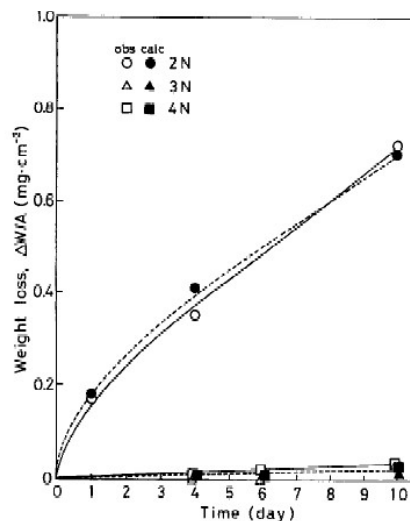


Figure 4 – Weight loss of alumina specimens [4]

Oda and Yoshia also tested the corrosion of alumina samples in aqueous solutions of 0.1 mol/kg HCl and 0.1 mol/kg H₂SO₄ at a range of sub- and supercritical temperatures. The test was conducted for a duration of 50 hours at temperatures of 240°C, 290°C, 340°C, 390°C, 500°C and at a pressure of 27 MPa. The three samples consisted of a 99.99% pure sample (TAI), a commercially available 99.7% alumina sample (ALC), and a zirconia toughened alumina sample (ZTA). Table 3 shows the compositions of the specimens. Weight loss of the specimens was measured, and is shown in Figure 5.

Table 3- Composition of alumina specimens [4]

	Al ₂ O ₃	ZrO ₂ (%)	Y ₂ O ₃ (%)	SiO ₂ (ppm)	MgO (ppm)	Fe ₂ O ₃ (ppm)	CaO (ppm)	TiO ₂ (ppm)
TAI	99.99	-	-	17	2	10	2	-
ALC	99.7	-	-	430	2700	700	180	50
ZTA	90	9.23	0.74	810	500	12200	170	130

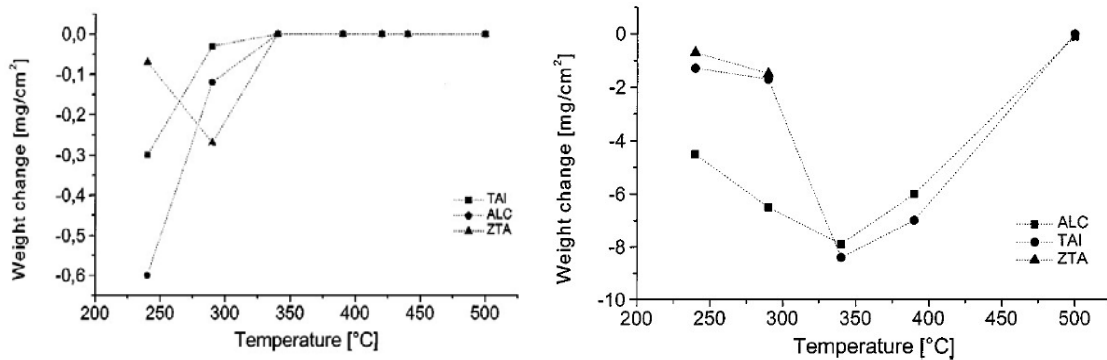


Figure 5- Weight loss of alumina specimens in HCl (left) and H₂SO₄ (right) solutions [4]

In HCl and H₂SO₄ solution, the weight loss of the samples diminishes as the temperature is increased above the supercritical point. This fact is very likely attributable to the lower solubility of the corrosion products as the density of water drops at higher temperature and the water transitions to the supercritical state. The specimens tested in the H₂SO₄ solution showed much higher weight loss, as sulfuric acid is more corrosive to high purity alumina when Al₂O₃ reacts with H₂SO₄ to form Al₂(SO₄)₃. Subcritical water has a high H⁺ and OH⁻ ion concentration, therefore any source of sulphate ion would create the corrosive environment equivalent to H₂SO₄ and cause the sulphation of alumina. Calcium sulphate in hard water could be a possible source of sulphate ion detrimental to an alumina tile.

ZTA was not tested in H₂SO₄ at temperatures beyond 290°C, but in the tests performed at 240°C and 290°C the ZTA sample exhibited better resistance to grain boundary attack by the H₂SO₄. This study concluded that the addition of zirconia improves the corrosion resistance of alumina ceramics. This observation was further supported by scanning electron microscope (SEM) micrographs of the ALC sample where less intergranular attack by H₂SO₄ was observed in comparison to the ALC sample. ZrO₂ strongly segregated to the grain boundaries, which appears to make the grain boundaries more resistant to corrosion.

3.2 Zirconia – ZrO₂

As seen in Table 1, zirconia has only 1/9th the thermal conductivity of alumina, which would enable a heat shielding tile of 1/9th the thickness of an equivalent alumina tile, making it a promising candidate. Zirconia has three stable crystal structures. It has a monoclinic structure at low temperatures, transforming to tetragonal at 1170°C, and to cubic at 2370°C. The transformation from tetragonal to monoclinic on cooling is martensitic (rapid, diffusionless and involving only small atomic displacements) and causes a substantial volume change, on the order of 3% - 5%. Since zirconia is a brittle ceramic, the tetragonal to monoclinic transformation causes cracking in zirconia when being cooled from elevated temperature. Addition of certain oxides, however, allows either the cubic or the tetragonal structure to be stabilized to room temperature and below. Pure tetragonal phase stabilized zirconia is referred to as tetragonal zirconia polycrystal (TZP). Partially stabilized zirconia (PSZ) has a cubic crystal matrix with some grains of tetragonal phase crystals dispersed within it. Both TZP and PSZ are commercially available, have good structural properties and several industrial uses.

Work by Schacht, Boukis, et al [5] tested ceria stabilized TZP (Ce-TZP), yttria PSZ (Y-PSZ) and magnesia partially stabilized zirconia (Mg-PSZ) in 0.1 mol/kg HCl, H₂SO₄, and H₃PO₄ aqueous solutions at pressures of 27 MPa and temperatures of 390°C for a duration of 50 hours. After exposure to the supercritical acidic aqueous solutions, the samples were examined by SEM and their weight change recorded, as shown in Table 4. In HCl solution, only the Ce-TZP sample performed well. With the Mg-PSZ sample, corrosion began at the grain boundaries where the impurity Mg₂SiO₄ became concentrated. As the grain boundaries were etched, the surface layer transformed to monoclinic phase (m-phase in Table 4) within a short period of time, causing intergranular microcracking of the surface layer and allowing penetration of the corrosive solution and ultimate disintegration of the sample as it underwent tetragonal to monoclinic phase transformation. The Mg,Y-PSZ sample performed much better, but still underwent a substantial transformation to the monoclinic phase. Its superior corrosion performance was attributed to its lower silicate impurity content. The Ce-TZP was largely immune to attack in HCl probably due to its low silicate impurity level.

Table 4- Zirconia corrosion test results after 50 hours [5]

Medium	HCL			H ₂ SO ₄			H ₃ PO ₄		
	Ce-TZP	Mg,Y-PSZ	Mg-PSZ	Ce-TZP	Mg,Y-PSZ	Mg-PSZ	Ce-TZP	Mg,Y-PSZ	Mg-PSZ
Weight Change (mg/cm ²)	<-0.1	0.3	-1	-52.3	-4.5	-6.6	0.1	0.1	0.2
m-phase after testing (vol %)	<2	31	93	33	92	98	<2	18	11
Initial m-phase (vol %)	0	15	8-9	0	15	8-9	0	15	8-9

The H₂SO₄ environment was caused serious degradation of all the samples and almost total transformation to the monoclinic phase on the surface of both the Mg-PSZ and Mg,Y-PSZ samples. Bulk penetration rate was low for both of these samples and that the monoclinic phase was confined to the surface, but given the large volume change in transformation to the

monoclinic phase, it is not clear how this can be a protective surface layer. The Ce-TZP breaks down by dissolution of the ceria surface layer and a tetragonal to monoclinic phase transformation on the surface, leading to fast penetration of the bulk of sample and total destruction. H_3PO_4 is much less destructive and all samples showed a small weight gain due to the formation of a protective zirconium phosphate surface layer. Some transformation to the monoclinic phase was detected, but the transformation was limited because of the adherent and protective zirconium phosphate layer.

The corrosion resistance in aggressive environments of the stabilized zirconia, like the alumina samples tested, is highly dependent on their purity, with any silica or silicate contaminant increasing corrosion. Contamination is much more problematic for the stabilized zirconia ceramics as any grain boundary attack disrupts the structural integrity of the samples and causes a destructive phase transformation. Therefore the use of such ceramics over alumina would be higher risk, and it would be extremely important that the water used in the reactor be uncontaminated by sulphides or chlorides.

3.3 Silica Glasses – SiO_2

Although borosilicate glasses are used by the nuclear industry to contain high level radioactive waste (HLW) for the purposes of underground burial, the corrosive environment experienced by such materials in that application is vastly different from that of a liner in a reactor core. The glasses containing HLW are built as a vitrified shell with the nuclear material embedded within and the entire shell then encased in a stainless steel drum [6]. Some water infiltration will occur but in a reactor the temperature, pressure and quantity of water would be far greater. Silicates are thermodynamically unstable in aqueous solution. Silica will dissolve in water by the hydration reaction [7][8][9]:



Or by the following reaction [10]:



Figure 6 shows calculated constant solubility curves, measured in grams SiO_2 per kilogram of H_2O , over temperature and pressure for quartz (crystalline silica) [8]. Temperatures in the range of 500°C - 700°C at a pressure of about 25 MPa, yield a solubility somewhere in the range of 0.05 to 0.1 grams of silica per kg of water for crystalline silica, while the solubility of amorphous silica may be as much as an order of magnitude higher [11]. Since the mass of water in the core would be far greater than the mass of the liner, the substantial amount of the liner would dissolve in the water within the core. Silica glasses also soften at temperatures 650°C - 900°C depending on the composition of the glass. Despite the better thermodynamic stability of borosilicate glasses, they are unsuitable for use in any supercritical water environment.

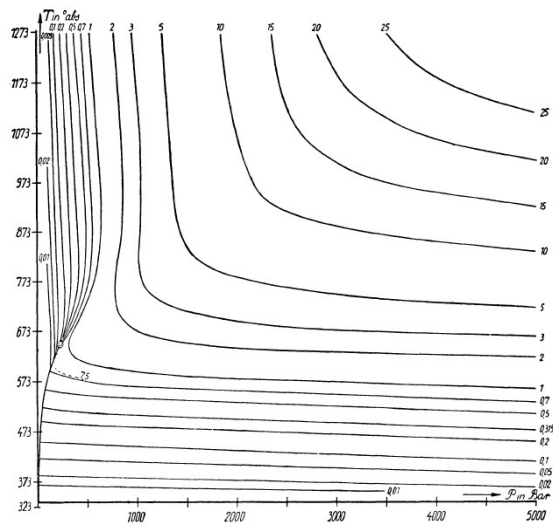


Figure 1- Solubility curves of quartz in water [8]

3.4 Silicon Carbide – SiC

Silicon carbide can be hydrolyzed in water and dissolved. The dissolution rate has been demonstrated to be higher in an alkaline solution than an acidic solution and greater in oxygenated water than non-oxygenated water [12]. Ultimately the dissolution of the silicon follows the same reaction path as for the dissolution of silica, producing $\text{Si}(\text{OH})_4$ (aq) or $2\text{H}^+ + \text{SiO}_3^{2-}$ [12]. Barringer, Lance, et al [13] studied the behaviour of SiC in supercritical water, and found corrosion to occur preferentially at the grain boundaries as evident in Figure 7. Similar to silica glasses, silicon based ceramics work poorly in a supercritical water situation, as corrosion at the silicon grain boundaries continues to break down the ceramic. Nagae, Yoshio, and Oda [14] also found SiC to undergo gradual deterioration in SCW without the formation of any protective layer. SiC has been proposed as a cladding material for nuclear fuel bundles [15] and it demonstrates good corrosion resistance in a short term test, but its solubility and lack of ability to form a protective surface layer leads to a linear weight loss making it a poor candidate for long term SCW exposure.

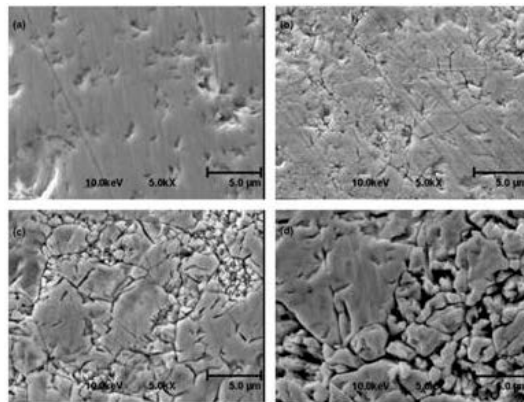


Figure 2 – Corrosion at grain boundaries in SiC [13]

3.5 Silicon Nitride – Si₃N₄

As with other silicon based ceramics, silicon nitride is not suitable for long term use as heat tile material in supercritical water. Silicon nitride is unstable in an oxidizing atmosphere, where a SiO₂ surface layer will form and then be hydrolyzed and dissolved. Despite this obvious drawback experimental studies are available on the performance of Si₃N₄ ceramic samples in supercritical water, which confirm that corrosion proceeds by the growth of a surface layer of silica followed by subsequent hydrolyzation and dissolution[11].

3.6 Sialon

Silicon aluminum oxygen nitrogen (sialon) compounds are essentially formed by a combination of alumina and silicon nitride. Their formation relies on the simultaneous crystal lattice substitutions of Al³⁺ for Si⁴⁺ and O²⁻ for N³⁻ in a silicon nitride crystal. Sialon is formed by liquid phase sintering of silicon nitride using metal oxide additives as sintering aids. At high temperatures, the sintering aids react to form an oxynitride liquid phase at the surfaces of the particles. Silicon nitride can crystallize in one of two forms, α-Si₃N₄ or β-Si₃N₄. β-Si₃N₄ is more stable at all temperatures, but α-Si₃N₄ can be formed under special conditions. The starting material is β-Si₃N₄ for β-sialons and typically α-Si₃N₄ for α-sialons, although α-sialons may also be made using amorphous silicon nitride as the starting material. A key distinguishing feature between the α- and β-sialons is that some of the liquid sintering phase solidifies to form a glassy phase at the grain boundaries in β-sialon. In α-sialons no grain boundary phase, or extremely little grain boundary phase, is present. Another key distinguishing feature is that the α-sialons have equiaxed grains whereas the β-sialons have an acicular grain structure. α/β-sialons are a composite mixture of the two crystals [16].

Sialons are known for their good high temperature strength, fracture toughness, low thermal expansion, hardness, and good corrosion resistance imparted by the aluminum and oxygen additions [3]. The lack of a grain boundary phase in the α-sialons tends to give them improved mechanical properties, particularly at high temperatures [16], but the crystal structure difference makes the distinction less clear.

Nagae et al. examined the corrosion resistance of three sialon compounds in supercritical water at 450°C and 45 MPa. The sample compositions are shown in Table 5. Y₂O₃ was used as a sintering aid in α- and α/β-sialons. The weight loss measurements after supercritical water exposure are shown in Figure 8 [10]. A corrosion resistant surface layer appears to have developed after 50 hour of the test. Due to the short duration of the test, it did not conclusively show that the surface layer formed was sufficiently protective to resist continued gradual attack. Being silicon nitride based, which is readily destroyed in SCW, it seems unlikely that sialon could offer corrosion resistance comparable to alumina, however given the lack of available data, sialon, particularly α-sialon, can be a candidate for further study with a test objective of conducting corrosion tests over a longer time period.

Table 5- Sialon specimen compositions [10]

Specimen	α -sialon	α/β -sialon	β -sialon
Composition formula	$Y_x(Si_{12-4.5x}, Al_{4.5x})(O_{1.5x}, N_{16-1.5x})$ $x=0.5$	$Y_x(Si_{12-4.5x}, Al_{4.5x})(O_{1.5x}, N_{16-1.5x})$ $x=0.2$	$Si_{6-z}Al_zO_zN_{8-z}$ $z=0.5$
Resulting composition	$Y_2(Si_{39}Al_9)(O_3N_{61})$	$Y_2(Si_{111}Al_{90})(O_{30}N_{157})$	$Si_{11}AlON_{15}$

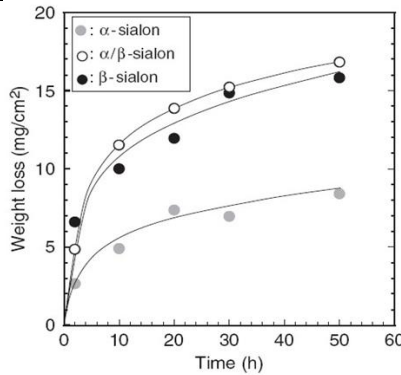


Figure 8 - Weight loss of sialon specimens [10]

3.7 Mullite – $3Al_2O_3 \cdot 2SiO_2$

Mullite is a stable intermediate phase in the alumina-silica system with the composition of $3Al_2O_3 \cdot 2SiO_2$. It is a naturally occurring mineral, but fairly rare, therefore it is normally synthetically prepared. It is commonly used as a refractory material and as such often used to line furnaces for the steel and glass making industries and for fabricating kiln fixtures in the ceramics industry. Nagae, Yoshio, and Oda[14] tested two compositions of mullite in supercritical water at 450°C and 45MPa, one with the stoichiometric ratio of 72 weight% alumina, 28 weight% silica and one with slightly silica rich (29 weight% silica). The mullite samples (72A, 71A) were tested along against silicon nitride, silicon carbide, and alumina samples (2N, 3N, 4N, sapphire in order of increasing purity). Figure 9 shows the weight loss.

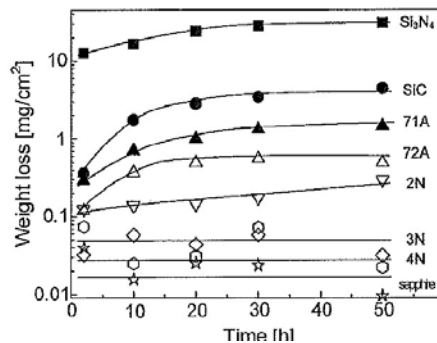


Figure 9 - Weight loss of ceramic samples over time [14]

As seen in this test, mullite performed better than the silicon nitride and silicon carbide, but not as well as the alumina samples. SEM images of the mullite showed that selective dissolution of the silica occurred in the surface layer, with simultaneous formation of boehmite ($Al(OH)_3$). Since the growth rate of the corroded layer diminished over time, the boehmite offered some

corrosion protection. Weight loss appears to level off, but the limited test time of 50 hours may not be sufficient. The study by Boukis et al [2] showed a protective layer of alumina formation, and found improved results with mullite-zirconia alloys. Mullite and mullite matrix composites, particularly mullite-zirconia composites, are candidates for further study. An advantage to mullite over alumina is its lower thermal conductivity (approximately 1/3rd that of alumina).

3.8 Aluminum Nitride – AlN

Aluminum nitride was demonstrated by Boukis et al [2] to be quite stable in supercritical water with 0.05 mol/kg HCl and 3% H₂O₂, but its stability is due to the formation of a protective alumina layer. Therefore long term corrosion performance of aluminum nitride may not surpass that of alumina. Aluminum nitride has a very high thermal conductivity (approximately nine times that of alumina) [2], therefore any tile made of AlN would need to be nine times the thickness of an equivalent alumina tile for the equivalent thermal impedance. This effectively rules it out as a candidate material.

4. Conclusions

High purity alumina (Al₂O₃) has excellent corrosion resistance and is the leading candidate material of the commonly available refractory ceramics. Its corrosion resistance degrades with the presence impurities, particularly silica, which tends to segregate to the grain boundaries making the alumina susceptible to grain boundary corrosion. The addition of zirconia (10%) to alumina, known as zirconia toughened alumina (ZTA), appears to make the material much more resistant to grain boundary attack, and therefore less sensitive to the presence of impurities. Stabilized zirconia (ZrO₂) can also provide excellent corrosion resistance, but only if no sulphates are present in the water. Similar to alumina, the corrosion resistance of zirconia is highly dependent on purity, with any silica or silicate contaminant significantly increasing corrosion rate. The risk of the stabilized zirconia is that they consist of a metastable phase or phases and any grain boundary corrosion could cause a catastrophic martensitic phase transformation to the monoclinic phase. The stabilized zirconia are worthy of further testing, their corrosive behaviour and long term phase stability will need to be carefully evaluated.

Mullite (3Al₂O₃•2SiO₂) appears to have a corrosion resistance that is inferior to alumina, but it forms a protective layer of either boehmite or alumina depending on the conditions. Mullite and the mullite composites are candidates for study, as it has a thermal conductivity that is about 1/3rd that of alumina. α -sialon is also a candidate for further study as it has demonstrated corrosion resistance over a short time period. β -sialon is attacked more severely in supercritical water and undergoes grain boundary corrosion.

Aluminum nitride (AlN) is quite corrosion resistant in SCW, but only because it forms a protective alumina layer, therefore its corrosion resistance will be no better than alumina. It also has a thermal conductivity that is about nine times that of alumina, so it is not suitable as a candidate insulation material. Silicon nitride, silicon carbide, and the silica glasses all corrode severely in SCW and can be ruled out as potential candidates.

5. References

- [1] Kritzer, Peter. "Corrosion in high-temperature and supercritical water and aqueous solutions: a review." *Journal of Supercritical Fluids* 29, no. 1-2 (2004): 1-29.
- [2] Boukis, Nikolaos, Nils Claussen, Klaus Ebert, Rolf Janssen, and Michael Schacht. "Corrosion Screening Tests of High-Performance Ceramics in Supercritical Water Containing Oxygen and Hydrochloric Acid." *Journal of the European Ceramic Society* 17, no. 1 (1997): 71-76.
- [3] Accuratus. *Ceramic Materials' Character*. 2002. <http://accuratus.com/materials.html>.
- [4] Oda, Kohei, and Tetsuo Yoshio. "Hydrothermal Corrosion of Alumina Ceramics." *Journal of the American Ceramic Society* 80, no. 12 (1997): 3233-3236.
- [5] Schacht, Michael, Nikolaos Boukis, and et al. "Corrosion of Zirconia Ceramics in Acidic Solutions at High Pressures and Temperatures." *Journal of the European Ceramic Society* 18, no. 16 (1998): 2373-2376.
- [6] Wicks, G. G. "Nuclear Waste Glasses: Corrosion Behaviour and Field Tests." In *Corrosion of Glass, Ceramics, and Ceramic Superconductors, Principles, Testing, Characterization, and Applications*, by David E. Clark and Bruce K. Zoitos. Noyes Publications, 1992.
- [7] Anderson, G. M., and C. Wayne Burnham. "The Solubility of Quartz in Supercritical Water." *American Journal of Science* 263, no. 6 (1965): 494-511.
- [8] Mosebach, Rudolf. "The Thermodynamic Behaviour of Quartz and Other Forms of Silica in Pure Water at Elevated Temperatures and Pressures with Conclusions on their Mechanism of Solution." *Journal of Geology* 65, no. 4 (1957): 347-363.
- [9] Wasserburg, G. T. "The Solubility of Quartz in Supercritical Water as a Function of Pressure." *Journal of Geology* 66, no. 5 (1958): 559-578.
- [10] Nagae, Masahiro, Yasunori Koyama, and et al. "Corrosion Behaviour of Sialon Ceramics in Supercritical Water." *Journal of the American Ceramic Society* 89, no. 11 (2006): 3550-3553.
- [11] Proverbi, Eduardo, Fabio Carassiti, and et al. "Low Temperature Oxidation of Silicon Nitride by Water in Supercritical Condition." *Journal of the European Ceramic Society* 16, no. 10 (1996): 1121-1126.
- [12] Hirayama, Hideo, Takashi Kawakubo, and et al. "Corrosion Behaviour of Silicon Carbide in 290C Water." *Journal of the American Ceramic Society* 72, no. 11 (1989): 2049-2053.
- [13] Barringer, E., and M. Lance. "Corrosion of CVD Silicon Carbide in 500C Supercritical Water." *Journal of the American Ceramic Society* 90, no. 1 (2007): 315-318.
- [14] Nagae, Masahiro, Tetsuo Yoshio, and Kohei Oda. "Corrosion Behavior of Structural Ceramics in Supercritical Water." *Advances in Science and Technology* 45 (2006): 173-177.
- [15] Kim, Weon-Ju, Ho Soo Hwang, and et al. "Corrosion behaviors of sintered and chemically vapor deposited silicon carbide ceramics in water at 360C." *Journal of Materials Science Letters* 22, no. 8: 581-584.
- [16] Cao, G. Z., and R. Metselaar. "- Sialon Ceramics: A Review." *Chemistry of Materials* 3, no. 2 (1991): 242-252.
- [17] Schacht, M., N. Boukis, and E. Dinjus. "Corrosion of alumina ceramics in acidic aqueous solutions at high temperatures and pressures." *Journal of Materials Science* 35, no. 24 (2000): 6251-6258.